

Rugged Metropolis sampling with simultaneous updating of two dynamical variables

Bernd A. Berg^{1,2} and Huan-Xiang Zhou^{1,2,3}

¹*Department of Physics, Florida State University, Tallahassee, Florida 32306-4350, USA*

²*School of Computational Science, Florida State University, Tallahassee, Florida 32306-4120, USA*

³*Institute of Molecular Biophysics, Florida State University, Tallahassee, Florida 32306-4380, USA*

(Received 7 February 2005; revised manuscript received 9 May 2005; published 21 July 2005)

The rugged Metropolis (RM) algorithm is a biased updating scheme which aims at directly hitting the most likely configurations in a rugged free-energy landscape. Details of the one-variable (RM₁) implementation of this algorithm are presented. This is followed by an extension to simultaneous updating of two dynamical variables (RM₂). In a test with the brain peptide Met-Enkephalin in vacuum RM₂ improves conventional Metropolis simulations by a factor of about 4. Correlations between three or more dihedral angles appear to prevent larger improvements at low temperatures. We also investigate a multihit Metropolis scheme, which spends more CPU time on variables with large autocorrelation times.

DOI: [10.1103/PhysRevE.72.016712](https://doi.org/10.1103/PhysRevE.72.016712)

PACS number(s): 05.10.Ln, 87.15.-v, 87.14.Ee

I. INTRODUCTION

Simulations of biomolecules are one of the major challenges in computational science. Rugged free-energy landscapes are typical for such systems. In this context a rugged Metropolis (RM) algorithm was introduced in Ref. [1]. The motivation of the RM algorithm was an elaboration of the funnel picture of protein folding, which was originally formulated by Bryngelson and Wolynes [2]. The RM algorithm uses a biased Metropolis algorithm, with the bias of the updating proposal obtained using data from previous simulations at higher temperatures. Although the possibility of constructing biased Metropolis algorithms has been known for many years [3] and these have occasionally been used in the statistical physics [4,5] and biochemical [6–8] literature, it seems that a systematic understanding of the possibilities of biased Metropolis procedures is still in its infancy. For instance, it was only recently noted [9] that biased one-variable updates allow one to imitate the heat-bath (Gibbs sampler) updates and can still be efficient when the conventional calculation of heat-bath probabilities becomes prohibitively slow.

The RM approach is distinct from generalized ensemble simulations. Generalized ensembles (for reviews and recent work see [10]) also use information from higher temperatures, but in an entirely different way. In a sense generalized ensembles build bridges in a rugged free-energy landscape, while the RM scheme aims to enhance the likelihood for a direct hit of the needle in the haystack. In fact, RM updates can be implemented within any generalized ensemble. In a test case of RM updates within a replica exchange simulation, the improvement was multiplicative [1].

The main technical challenge within the RM scheme is to obtain, from available time series data, estimates of the multivariable probability densities (PD's) in a form that allows for their fast numerical evaluation. So far, this has only been achieved for one-variable PD's, resulting in the RM₁ update scheme. However, it is well known that many degrees of freedom in a protein molecule are coupled. In addition, one needs multivariable moves to avoid steric clashes [11] (cf. [8] and references therein for more recent literature). As a

next approximation to the desired RM probabilities, in this paper we deal with PD's of two variables to develop and test the corresponding RM₂ update scheme.

In the present paper all our Monte Carlo (MC) simulations are done in the canonical ensemble for the brain peptide Met-Enkephalin in vacuum, which has been a frequently used test case since its initial numerical investigation in Ref. [12]. For this (artificial) system the coil-globule transition temperature is at $T_\theta \approx 295$ K and the folding temperature is at $T_f \approx 230$ K according to Ref. [13]. Long-living traps are found at the glass transition temperature, which is for Met-Enkephalin below the folding temperature at $T_g \approx 180$ K [14]. In our simulations we cover a range from 400 K down to 220 K and measure integrated autocorrelation times (see, e.g., Ref. [15] for the definition) to determine the performance of our algorithms.

In Sec. II we review the RM scheme and its RM₁ approximation, filling in many details which inevitably had to be omitted in the letter format of Ref. [1]. On the fly we also investigate a multihit updating procedure, which spends more computer time on variables with large integrated autocorrelation times. In Sec. III we introduce and test a RM₂ scheme. A summary and conclusions follow in Sec. IV.

II. RM AND THE RM₁ APPROXIMATION

We consider biomolecule models for which the energy E is a function of a number of dynamical variables v_i , $i = 1, \dots, n$. The fluctuations in the Gibbs canonical ensemble are described by a PD $\rho(v_1, \dots, v_n; T)$, where T is the temperature. To be definite, we use in the following the all-atom energy function ECEPP/2 (empirical conformational energy program for peptides) [16]. Our dynamical variables v_i are the dihedral angles, each chosen to be in the range $-\pi \leq v_i < \pi$, so that the volume of the configuration space is $K = (2\pi)^n$. Details of the energy functions are expected to be irrelevant for the algorithmic questions addressed here. Our test case will be the small brain peptide Met-Enkephalin, which features 24 dihedral angles as dynamical variables; see Table I (the conventions follow Ref. [17], which differs from

TABLE I. Acceptance rates for dihedral angle movements. They are accurate to about ± 1 in the last digit.

| Var | Angle | Residues | 400 K | 300 K | 300 K |
|----------|----------|----------|--------|-------|-----------------|
| | | | Metro. | Metro | RM ₁ |
| v_1 | χ^1 | Tyr-1 | 0.107 | 0.070 | 0.272 |
| v_2 | χ^2 | Tyr-1 | 0.182 | 0.128 | 0.343 |
| v_3 | χ^6 | Tyr-1 | 0.497 | 0.377 | 0.680 |
| v_4 | ϕ | Tyr-1 | 0.392 | 0.340 | 0.547 |
| v_5 | ψ | Gly-2 | 0.096 | 0.044 | 0.139 |
| v_6 | ω | Gly-2 | 0.049 | 0.034 | 0.416 |
| v_7 | ϕ | Gly-2 | 0.112 | 0.045 | 0.076 |
| v_8 | ψ | Gly-3 | 0.106 | 0.038 | 0.064 |
| v_9 | ω | Gly-3 | 0.041 | 0.025 | 0.301 |
| v_{10} | ϕ | Gly-3 | 0.088 | 0.035 | 0.070 |
| v_{11} | ψ | Phe-4 | 0.115 | 0.040 | 0.077 |
| v_{12} | ω | Phe-4 | 0.047 | 0.030 | 0.368 |
| v_{13} | χ^1 | Phe-4 | 0.109 | 0.086 | 0.277 |
| v_{14} | χ^2 | Phe-4 | 0.192 | 0.166 | 0.403 |
| v_{15} | ϕ | Phe-4 | 0.082 | 0.042 | 0.139 |
| v_{16} | ψ | Met-5 | 0.122 | 0.063 | 0.156 |
| v_{17} | ω | Met-5 | 0.062 | 0.047 | 0.573 |
| v_{18} | χ^1 | Met-5 | 0.117 | 0.092 | 0.362 |
| v_{19} | χ^2 | Met-5 | 0.159 | 0.121 | 0.585 |
| v_{20} | χ^3 | Met-5 | 0.269 | 0.211 | 0.709 |
| v_{21} | χ^4 | Met-5 | 0.455 | 0.385 | 0.833 |
| v_{22} | ϕ | Met-5 | 0.129 | 0.086 | 0.258 |
| v_{23} | ψ | Met-5 | 0.378 | 0.267 | 0.469 |
| v_{24} | ω | Met-5 | 0.114 | 0.096 | 0.873 |
| E | | | 0.168 | 0.119 | 0.375 |

[12]). Besides the ϕ and ψ angles, we keep also the ω angles unconstrained, which are usually restricted to $[\pi - \pi/9, \pi + \pi/9]$. This allows us to illustrate the RM idea for a particularly simple case.

The Metropolis importance sampling would be perfected if we could propose new configurations $\{v'_i\}$ with their canonical PD. This is not possible as no Metropolis simulation would be necessary if the canonical PD were known. But conventional Metropolis simulations work well at sufficiently high temperatures T' and can thus provide an *estimate* $\bar{\rho}(v_1, \dots, v_n; T')$ of the PD $\rho(v_1, \dots, v_n; T')$. Due to the funnel picture, we expect that such an *estimate* can be used to feed useful information into the simulation at a sufficiently close-by lower temperature $T < T'$ [1]. The idea of the RM scheme is to propose a transition from a configuration $\{v_i\}$ to a new configuration $\{v'_i\}$ with the PD $\bar{\rho}(v'_1, \dots, v'_n; T')$ and to accept it with the probability

$$P_a = \min \left[1, \frac{\exp(-\beta E') \bar{\rho}(v_1, \dots, v_n; T')}{\exp(-\beta E) \bar{\rho}(v'_1, \dots, v'_n; T')} \right], \quad (1)$$

where $\beta = 1/(kT)$. This equation biases the *a priori* probability of each dihedral angle with an estimate of its PD from a

higher temperature. Arbitrary generalized ensembles can be treated similarly by replacing $\exp(-\beta E')$ and $\exp(-\beta E)$ in Eq. (1) by the appropriate probabilities $P_g(E')$ and $P_g(E)$ of the generalized ensemble.

For a range of temperatures

$$T_1 > T_2 > \dots > T_r > \dots > T_{f-1} > T_f, \quad (2)$$

the simulation at the highest temperature T_1 is performed with the usual Metropolis algorithm and the results are used as input for the simulation at T_2 . The estimated PD $\bar{\rho}(v_1, \dots, v_n; T_{r-1})$ is expected to be a useful approximation of $\rho(v_1, \dots, v_n; T_r)$, therefore allowing the scheme to zoom in on the native structure that is dominant at the physically relevant final temperature T_f .

To get things started, we need to construct an estimator $\bar{\rho}(v_1, \dots, v_n; T_r)$ from the numerical data of the RM simulation at temperature T_r . Although this is neither simple nor straightforward, a variety of approaches offer themselves to define and refine the desired estimators.

In Ref. [1] the approximation

$$\bar{\rho}(v_1, \dots, v_n; T_r) = \prod_{i=1}^n \bar{\rho}_i^1(v_i; T_r) \quad (3)$$

was investigated, where $\bar{\rho}_i^1(v_i; T_r)$ are estimators of reduced one-variable PD's defined by

$$\rho_i^1(v_i; T) = \int_{-\pi}^{+\pi} \prod_{j \neq i} dv_j \rho(v_1, \dots, v_n; T). \quad (4)$$

The resulting algorithm, called RM₁, constitutes the simplest RM scheme possible.

Let us fill in the details of the RM₁ implementation [1]. To update with the RM₁ weights it is convenient to rely on the cumulative distribution functions defined by

$$F_i(v) = \int_{-\pi}^v dv' \rho_i^1(v'). \quad (5)$$

The estimate of F_{10} , the cumulative distribution function for the dihedral angle Gly-3 ϕ (v_{10}), from the vacuum simulations at our highest temperature, $T_1 = 400$ K, is shown in Fig. 1 (this is the same angle for which histograms at 400 K and 300 K are shown in Ref. [1]). For our plots in the present paper we use degrees, while we use radians in our theoretical discussions and in the computer programs. Figure 1 is obtained by sorting all n_{dat} values of v_{10} in our time series in ascending order and increasing the values of F_{10} by $1/n_{\text{dat}}$ whenever a measured value of v_{10} is encountered. Using a heap-sort approach, the sorting is done in $n_{\text{dat}} \log_2(n_{\text{dat}})$ steps (see, e.g., Ref. [15]).

Next we divide the ordinate between 0 and 1 into n_{tab} equal segments. The value of n_{tab} has to be small enough that a table of size $n \times n_{\text{tab}}$ fits conveniently into the computer RAM. For each integer $j = 1, \dots, n_{\text{tab}}$ the value $F_{i,j} = j/n_{\text{tab}}$ defines a unique value $v_{i,j}$ through $F_{i,j} = F_i(v_{i,j})$ as is indicated in the figure (for which $i = 10$). Furthermore, for each choice of a dihedral angle (i.e., a particular value of i) we define the differences

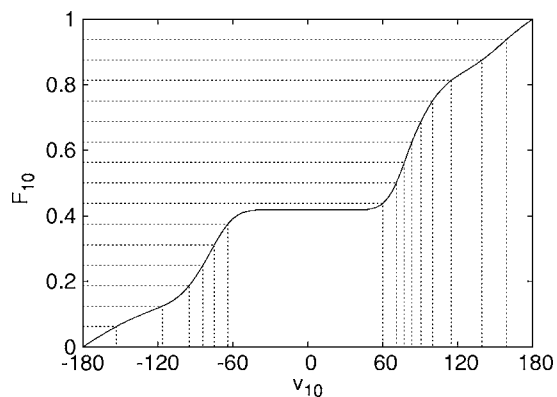


FIG. 1. Estimate of the cumulative distribution function for the Met-Enkephalin dihedral angle v_{10} (Gly-3 ϕ) at 400 K.

$$\Delta v_{i,j} = v_{i,j} - v_{i,j-1} \text{ with } v_{i,0} = -\pi. \quad (6)$$

The grid in Fig. 1 shows the discretization for the variable v_{10} and the choice $n_{\text{tab}}=16$. While the discretization for F_{10} on the ordinate is uniformly spaced, widely varying intervals are obtained for v_{10} on the abscissa. The Metropolis procedure for one update of a dihedral angle v_i is now specified as follows:

- (i) Place the present angle v_i on the discretization grid—i.e., find the integer j through the relation $v_{i,j-1} \leq v_i < v_{i,j}$. For one-variable updates j is available in the computer memory if it is stored at the previous update. Otherwise, j can be recalculated in n_2 steps for the choice $n_{\text{tab}}=2^{n_2}$ [9].
- (ii) Pick an integer j' uniformly distributed in the range 1 to n_{tab} .
- (iii) Propose $v'_i = v_{i,j'-1} + x' \Delta v_{i,j'}$, where $0 \leq x' < 1$ is a uniformly distributed random number.
- (iv) Accept v'_i with the probability

$$p_a = \min \left[1, \frac{\exp(-\beta E') \Delta v_{i,j'}}{\exp(-\beta E) \Delta v_{i,j}} \right]. \quad (7)$$

It is through the widely varying ratios $\Delta v_{i,j'}/\Delta v_{i,j}$ that importance sampling for the rugged variables becomes improved. Back to our illustration in Fig. 1: The short and long intervals on the abscissa are proposed with equal probabilities; i.e., the *a priori* probability density for our angle is high in short intervals and low in long intervals. The CPU time consumption of the RM₁ scheme is practically identical with that of the conventional Metropolis algorithms, because the bulk of the CPU time is spend on the calculation of the new energy E' .

A. Numerical results

The performance of the RM₁ algorithm is tested at 300 K using input from a simulation at 400 K. The temperature of 400 K is high enough so that the conventional Metropolis algorithm is efficient, while it is low enough to provide useful input for the simulation at 300 K, a temperature at which one experiences a considerable slowing down in a conventional Metropolis simulation of Met-Enkefalin.

Our Metropolis simulations are performed with a variant

of SMMP (simple molecular mechanics for proteins) [17]. For each simulation a time series of $2^{17}=131\,072$ configurations is kept, sampling every 32 sweeps. A sweep is defined by updating each dihedral angle once, which we do in the sequential order of the angles listed in Table I. Usually sequential updating is more efficient than random updating [15]. Before starting with the measurements, $2^{18}=262\,144$ sweeps are performed for reaching equilibrium. Thus, the entire simulation at one temperature uses $2^{18}+32 \times 2^{17}=4\,456\,448$ sweeps. On a 1.9-GHz Athlon PC this takes under 12 h. For each dihedral angle the acceptance rate of the Metropolis algorithm was monitored at run time and, following the recipes of [15], the integrated autocorrelation time τ_{int} is calculated from the recorded time series.

Acceptance rates for dihedral angle movements are compiled in Table I. For the energy entry it is the ratio of all accepted over all proposed moves. Results are given for simulations with the conventional Metropolis algorithm at 400 K and 300 K and for the RM₁ simulations at 300 K. The RM₁ updating uses a discretization with $n_{\text{tab}}=2^7=128$ from the 400 K Metropolis data. Acceptance rates greater than 0.3 are desirable [15]. From the table we notice that the acceptance rates vary greatly from angle to angle. For the Metropolis simulation the values are in the interval [0.041, 0.497] at 400 K and in [0.025, 0.387] at 300 K. For both temperatures v_9 corresponds to the lowest value, while v_3 and v_{21} correspond to the highest values.

Our RM₁ updating at 300 K increases the acceptance rate for each angle, often even beyond the Metropolis acceptance rate at 400 K, as is obvious from the average value listed for the energy. A second look reveals that the increase in the acceptance rate varies greatly from angle to angle. While for some angles the problem of low acceptance rates is entirely solved, for others the improvement remains modest. For instance, for all ω angles the increase is dramatic—e.g., from 0.034 to 0.416 for v_6 . Angles with little improvements are v_7 (0.045 \rightarrow 0.076), v_8 (0.038 \rightarrow 0.064), v_{10} (0.035 \rightarrow 0.070), and v_{11} (0.040 \rightarrow 0.077). Better, but still not particularly impressive, is the increase in the acceptance rates of v_5 , v_{15} , and v_{16} . All these are ϕ and ψ angles around C $_{\alpha}$ atoms. For all other angles RM₁ updating has moved the acceptance rate above or at least close to 0.3.

The improvement for ω angles is most easily understood. Figure 2 shows the cumulative distribution function for v_9 (Gly-2 ω) at 400 K, which is the angle of lowest acceptance rate in the conventional Metropolis updating. This distribution function corresponds to a histogram narrowly peaked around $\pm\pi$, which is explained by the specific electronic hybridization of the CO—N peptide bond. From the grid shown in Fig. 2 it is seen that the RM₁ updating concentrates the proposal for this angle in the range slightly above $-\pi$ and slightly below $+\pi$. Thus the procedure has a similar effect as the often used restriction to the range $[\pi-\pi/9, \pi+\pi/9]$, which is also the default implementation in SMMP (the range $[\pi, \pi+\pi/9]$ is, of course, $[-\pi, -\pi+\pi/9]$ in our plots).

Although acceptance rates give some insights, the decisive quantity for the performance of an algorithm is the more difficult to calculate integrated autocorrelation time τ_{int} . To achieve a predefined accuracy, the computer time needed is directly proportional to τ_{int} .

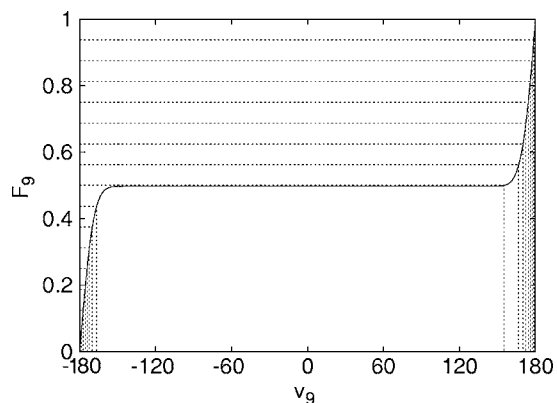


FIG. 2. Estimate of the cumulative distribution function for the Met-Enkephalin dihedral angle v_9 (Gly-2 ω) at 400 K.

In Table II the integrated autocorrelation times are compiled for all angles and for the energy. The values are statistically consistent with those of Ref. [1]. Deviations are due to reruns and using different procedures for estimating integrated autocorrelation times. In all tables they are given in units of 32 sweeps, as this is the step size of our MC time series. Error bars are shown in parentheses. For these calcu-

TABLE II. Integrated autocorrelation times for dihedral angle movements in units of 32 sweeps.

| Var | 400 K | 300 K | 300 K | 300 K |
|----------|-----------|------------|-----------------|-----------------|
| | Metro | Metro | RM ₁ | RM ₂ |
| v_1 | 2.11 (06) | 15.2 (1.5) | 9.07 (58) | 6.03 (47) |
| v_2 | 1.18 (02) | 2.70 (16) | 1.63 (09) | 1.70 (12) |
| v_3 | 1.03 (01) | 2.18 (14) | 1.26 (04) | 1.24 (04) |
| v_4 | 1.44 (03) | 4.44 (23) | 3.28 (21) | 2.82 (14) |
| v_5 | 5.44 (20) | 54.5 (5.4) | 26.3 (1.5) | 20.0 (1.3) |
| v_6 | 2.95 (07) | 23.3 (2.7) | 8.65 (58) | 6.00 (34) |
| v_7 | 5.83 (29) | 103 (14) | 52.9 (4.3) | 24.3 (1.3) |
| v_8 | 7.36 (22) | 125 (12) | 74.2 (6.9) | 35.0 (2.7) |
| v_9 | 4.39 (13) | 32.0 (2.2) | 14.2 (1.0) | 8.84 (48) |
| v_{10} | 9.08 (88) | 124 (12) | 80.6 (6.9) | 34.3 (2.8) |
| v_{11} | 5.39 (45) | 105 (08) | 72.4 (5.5) | 31.3 (1.9) |
| v_{12} | 3.37 (08) | 15.6 (1.5) | 5.68 (39) | 3.92 (17) |
| v_{13} | 1.81 (05) | 8.79 (46) | 5.69 (54) | 3.59 (22) |
| v_{14} | 1.15 (02) | 1.65 (10) | 1.40 (07) | 1.26 (06) |
| v_{15} | 6.72 (28) | 105 (12) | 45.6 (2.7) | 27.5 (4.5) |
| v_{16} | 9.28 (28) | 133 (09) | 75.2 (5.2) | 33.9 (2.1) |
| v_{17} | 1.90 (04) | 9.69 (79) | 3.89 (36) | 2.29 (08) |
| v_{18} | 1.66 (05) | 12.0 (1.6) | 6.48 (78) | 5.11 (28) |
| v_{19} | 1.17 (02) | 1.65 (08) | 1.16 (03) | 1.17 (03) |
| v_{20} | 1.02 (01) | 1.08 (02) | 1.03 (02) | 1.02 (02) |
| v_{21} | 1.00 (01) | 1.00 (01) | 1.00 (01) | 1.02 (01) |
| v_{22} | 3.20 (12) | 35.9 (4.0) | 18.2 (1.2) | 12.0 (0.8) |
| v_{23} | 1.50 (04) | 20.3 (1.8) | 11.0 (0.6) | 5.96 (35) |
| v_{24} | 1.07 (02) | 1.22 (05) | 1.00 (01) | 1.00 (01) |
| E | 4.89 (21) | 50.7 (5.0) | 26.0 (1.4) | 14.2 (0.7) |

lations we use the routines of Ref. [15] together with a jackknife error analysis as explained there. The angles $v_7, v_8, v_{10}, v_{11}, v_{15},$ and v_{16} exhibit autocorrelation times >100 in the conventional Metropolis simulation at 300 K. Note that four of these are those with the worst improvement of acceptance rates when moving to the RM₁ updating, while the remaining two belong to the subsequent group with still rather poor improvement.

The increase in magnitude in the autocorrelation times for these six angles is remarkable when the temperature of the conventional Metropolis simulation is lowered from 400 K to 300 K. This shows that the standard Metropolis algorithm is efficient at 400 K but not so at 300 K. On the other hand, the distribution of the variables is not dramatically changed, at least to the extent that this can be judged from one-variable histograms, as is illustrated in Ref. [1] for v_{10} . This is the reason why the 400 K simulation provides useful input for the RM₁ simulation at 300 K.

The RM₁ updating reduces the integrated autocorrelation times at 300 K by factors of about 2—for instance, for v_7 from 103 to 53. The τ_{int} values vary greatly from angle to angle. While some angles show no autocorrelations after 32 sweeps ($\tau_{\text{int}}=1$ or close to it), the largest value on record for RM₁ updating at 300 K is $\tau_{\text{int}}=80\pm 7$ for v_{10} (down from 124 for Metropolis updating at 300 K). That the RM₁ updating does not reduce the large autocorrelation times more efficiently has obviously to do with correlations between different angles. Notably even moves of some of the ω angles, like v_9 with $\tau_{\text{int}}=14.2\pm 1.0$, appear considerably correlated with the rest of the molecule. RM variants which move several dynamical variables collectively are required, and our RM₂ implementation for simultaneous updates of two dihedral angles is discussed in Sec. III. First let us address a multihit Metropolis procedure.

B. Multihit updating

Our sequential updating hits each angle once. The greatly varying integrated autocorrelation times of Table II suggest that the computer time may be more efficiently used by performing several Metropolis hits for variables with large integrated autocorrelation times, to be called “bad” variables in the following.

To find an optimal choice for the number of hits per variable requires some thought. At 300 K the integrated autocorrelation times of the dihedral angles vary between $\tau_{\text{int}}=1$ and $\tau_{\text{int}}\approx 133$ for the conventional Metropolis updating and still between $\tau_{\text{int}}=1$ and $\tau_{\text{int}}\approx 80$ for the RM₁ algorithm. It is certainly not a good idea to choose the number of hits per variable in proportion to τ_{int} , because we expect correlations between angles to be the main obstacle for reducing large integrated autocorrelation times. A scheme with a large number of hits mimics the heat-bath algorithm (e.g., Ref. [15]), which sets the upper bound to the gain in performance, but does not resolve the problem of correlations between angles. So a modest increase in the number of hits per bad variable may increase the performance of the updating, while a further increase will result in the contrary.

A guideline for choosing the number of hits is obtained from the observation that the previously obtained acceptance

TABLE III. Multihit performance.

| Var | 48 | 400 K | 300 K | 39 | 300 K | 300 K |
|----------|------|-----------|------------|------|-----------------|-----------------|
| | hits | Metro | Metro | hits | RM ₁ | RM ₂ |
| v_1 | 2 | 2.05 (07) | 14.2 (1.1) | 1 | 7.29 (52) | 5.66 (42) |
| v_2 | 1 | 1.37 (03) | 3.29 (23) | 1 | 1.56 (04) | 1.91 (05) |
| v_3 | 1 | 1.04 (04) | 2.15 (10) | 1 | 1.39 (04) | 1.51 (06) |
| v_4 | 1 | 1.47 (03) | 5.49 (57) | 1 | 2.74 (12) | 3.09 (16) |
| v_5 | 3 | 3.73 (08) | 48.1 (5.7) | 2 | 21.8 (1.7) | 20.3 (1.0) |
| v_6 | 1 | 4.19 (09) | 19.3 (1.2) | 1 | 7.12 (35) | 5.11 (22) |
| v_7 | 4 | 3.96 (21) | 61.7 (3.5) | 4 | 42.3 (2.9) | 20.7 (1.2) |
| v_8 | 4 | 5.06 (19) | 81.8 (5.2) | 4 | 50.5 (4.1) | 24.1 (1.2) |
| v_9 | 2 | 4.21 (13) | 25.0 (1.6) | 1 | 12.7 (1.0) | 8.14 (47) |
| v_{10} | 4 | 5.28 (20) | 86.1 (6.4) | 4 | 48.0 (4.4) | 24.7 (1.6) |
| v_{11} | 4 | 3.72 (14) | 81.1 (7.2) | 4 | 53.7 (4.8) | 25.5 (1.4) |
| v_{12} | 2 | 3.04 (13) | 11.3 (0.6) | 1 | 4.82 (42) | 4.61 (26) |
| v_{13} | 1 | 2.39 (05) | 9.36 (96) | 1 | 4.36 (29) | 3.45 (26) |
| v_{14} | 1 | 1.34 (03) | 2.03 (15) | 1 | 1.23 (03) | 1.28 (03) |
| v_{15} | 4 | 4.65 (16) | 61.1 (4.4) | 2 | 35.5 (3.2) | 20.3 (1.0) |
| v_{16} | 4 | 6.29 (20) | 86.7 (8.5) | 2 | 61.5 (5.0) | 29.5 (1.9) |
| v_{17} | 1 | 2.86 (06) | 7.48 (42) | 1 | 3.16 (30) | 2.18 (07) |
| v_{18} | 1 | 2.03 (05) | 11.7 (1.1) | 1 | 7.79 (91) | 6.48 (51) |
| v_{19} | 1 | 1.64 (04) | 2.57 (15) | 1 | 1.16 (02) | 1.32 (03) |
| v_{20} | 1 | 1.09 (01) | 1.21 (02) | 1 | 1.01 (01) | 1.02 (01) |
| v_{21} | 1 | 1.00 (01) | 1.02 (02) | 1 | 1.00 (01) | 1.00 (01) |
| v_{22} | 2 | 2.98 (08) | 26.2 (1.8) | 1 | 19.2 (1.6) | 13.9 (0.9) |
| v_{23} | 1 | 1.51 (05) | 13.3 (1.1) | 1 | 11.4 (1.0) | 5.60 (31) |
| v_{24} | 1 | 1.44 (03) | 1.63 (04) | 1 | 1.02 (01) | 1.03 (02) |
| E | | 4.25 (17) | 32.9 (1.4) | | 24.9 (2.2) | 14.7 (1.3) |

rates per update attempt do not change when performing multiple hits. It appears reasonable to increase the hits of bad variables while bounding the number of hits times the acceptance rate by 0.3 from above. As the acceptance rates change considerably when switching from regular Metropolis to RM₁ updating, we employ different schemes for the two cases. Results for the two different multihit schemes are collected in Table III.

The numbers in the first “hits” column are used for the regular Metropolis updating. They are arranged to add up to 48—i.e., twice the total number of variables. The additional computer time needed is balanced by reducing the number of sweeps between measurements from 32 to 16 (a sweep is now defined by applying the new updating procedure in sequential order once to each angle). By comparing Tables II and III we see that the multihit updating improves the Metropolis algorithm at 300 K considerably: the integrated autocorrelation time for the energy is down by about 40%.

The numbers in the second “hits” column are used for RM₁ and RM₂ updating. As RM₁ updating increases acceptance rates already significantly, there is little opportunity for additional improvements due to multiple hits. By that reason the numbers of the column add only up to 39 hits per sweep. This is balanced by reducing the number of sweeps between measurements from 32 to 20 (the integer nearest to 32

× 24/39). There are still significant decreases in autocorrelations times for the bad variables, but the indicator for overall performance—the integrated autocorrelation time of the energy—shows only a modest 5% decrease when comparing to RM₁ without multiple hits and practically no change for RM₂ updating, introduced next. The apparent reason is that these updating schemes are already much closer to a heat-bath scenario, so that the improvement due to multiple hits becomes offset by the additional computer time needed.

III. RM₂ APPROXIMATION

We now generalize the RM₁ scheme of Eq. (7) to the simultaneous updating of two dihedral angles. For $i_1 \neq i_2$ the reduced two-variable PD's are defined by

$$\rho_{i_1, i_2}^2(v_{i_1}, v_{i_2}; T) = \int_{-\pi}^{+\pi} \prod_{j \neq i_1, i_2} dv_j \rho(v_j, \dots, v_n; T). \quad (8)$$

The one-variable cumulative distribution functions F_{i_1} and the discretization $v_{i_1, j}, j=0, \dots, n_{\text{tab}}$ are already given by Eqs. (5) and (6). We define conditional cumulative distribution functions by

$$F_{i_1, i_2; j}(v) = \int_{-\pi}^v dv_{i_2} \int_{v_{i_1, j-1}}^{v_{i_1, j}} dv_{i_1} \rho_{i_1, i_2}^2(v_{i_1}, v_{i_2}), \quad (9)$$

for which the normalization $F_{i_1, i_2; j}(\pi) = 1/n_{\text{tab}}$ holds. To extend the RM₁ updating to two variables we define for each integer $k=1, \dots, n_{\text{tab}}$ the value $F_{i_1, i_2; j, k} = k/(n_{\text{tab}})^2$. Next we define $v_{i_1, i_2; j, k}$ through $F_{i_1, i_2; j, k} = F_{i_1, i_2; j}(v_{i_1, i_2; j, k})$ and also the differences

$$\Delta v_{i_1, i_2; j, k} = v_{i_1, i_2; j, k} - v_{i_1, i_2; j, k-1} \text{ with } v_{i_1, i_2; j, 0} = -\pi. \quad (10)$$

The RM₂ Metropolis procedure for the simultaneous update of (v_{i_1}, v_{i_2}) is then specified as follows.

(i) Find the grid index j for the present angle v_{i_1} through $v_{i_1, j-1} \leq v_{i_1} \leq v_{i_1, j}$, just like for RM₁ updating.

(ii) Find the grid index k for the present angle v_{i_2} through $v_{i_1, i_2; j, k-1} \leq v_{i_2} \leq v_{i_1, i_2; j, k}$.

(iii) Pick two integers j' and k' , each uniformly distributed in the range from 1 to n_{tab} . (This could be extended to cover asymmetric ranges $n_{\text{tab}}^1 \times n_{\text{tab}}^2$.)

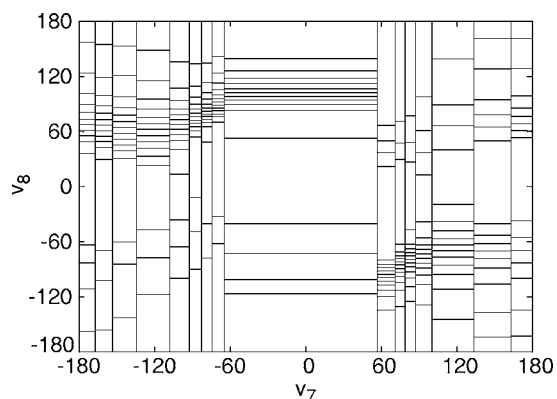
(iv) Propose $v'_{i_1} = v_{i_1, j'-1} + x'_1 \Delta v_{i_1, j'}$, where $0 \leq x'_1 < 1$ is a uniformly distributed random number.

(v) Propose $v'_{i_2} = v_{i_1, i_2; j', k'-1} + x'_2 \Delta v_{i_1, i_2; j', k'}$, where $0 \leq x'_2 < 1$ is a second uniformly distributed random number.

(vi) Accept (v'_{i_1}, v'_{i_2}) with the probability

$$p'_a = \min \left[1, \frac{\exp(-\beta E') \Delta v_{i_1, j'} \Delta v_{i_1, i_2; j', k'}}{\exp(-\beta E) \Delta v_{i_1, j} \Delta v_{i_1, i_2; j, k}} \right]. \quad (11)$$

As before, estimates of the conditional cumulative distribution functions and the intervals $\Delta v_{i_1, i_2; j, k}$ are obtained from the conventional Metropolis simulation at 400 K. In the following we focus on the pairs (v_7, v_8) , (v_{10}, v_{11}) , and (v_{15}, v_{16}) . These angles correspond to the largest integrated autocorrelation times of the RM₁ procedure and are expected

FIG. 3. Areas of equal probabilities (sorting v_7 then v_8).

to be strongly correlated with one another because they are pairs of dihedral angles around a C_α atom.

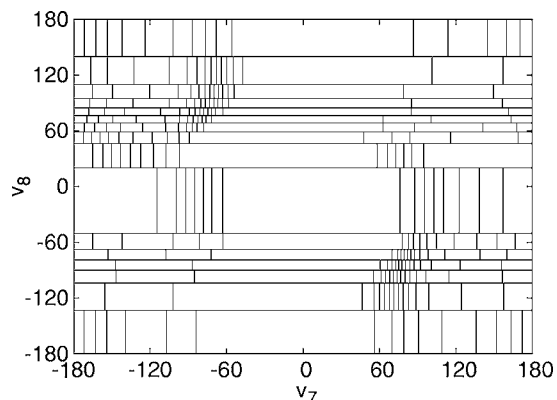
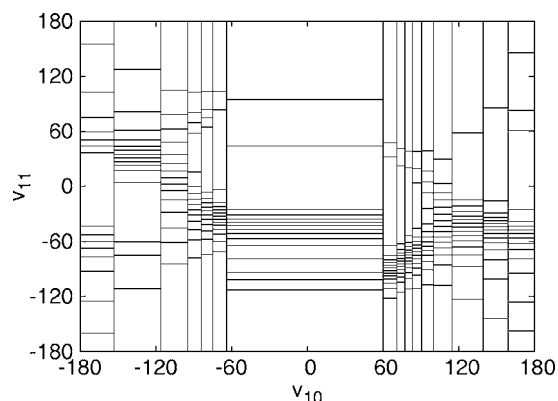
The bias of the acceptance probability given in Eq. (11) is governed by the areas

$$\Delta A_{i_1, i_2, j, k} = \Delta v_{i_1, j} \Delta v_{i_2, j, k}.$$

For $i_1=6$ and $i_2=7$ our 400 K estimates of these areas are depicted in Fig. 3. For the RM_2 procedure these areas take the role which the intervals on the abscissa of Fig. 1 play for RM_1 updating. The small and large areas are proposed with equal probabilities, so the *a priori* probability for our two angles is high in a small area and low in a large area. In Fig. 3 the largest area is 503.4 times the smallest area. Areas of high probability correspond to allowed regions in the Ramachandran map of a Gly residue [18].

Note that the order of the angles matters. The difference between Figs. 3 and 4 is that we plot in Fig. 3 the areas $A_{7,8;j,k}$ and in Fig. 4 the areas $A_{8,7;j,k}$ while the labeling of the axes is identical. This means that for Fig. 3 sorting is first done on the angle v_7 (regardless of the value of v_8) and then done on v_8 for which the corresponding value of v_7 is within a particular bin Δv_7 , but for Fig. 4 it is first done one v_8 and then on v_7 . In Fig. 4 the largest area is 396.4 times the smallest area.

Figures 5 and 6 give plots for the (v_{10}, v_{11}) and (v_{15}, v_{16}) pairs in which the angle with the smaller subscript is sorted first. The ratio of the largest area over the smallest area is

FIG. 4. Areas of equal probabilities (sorting v_8 then v_7).FIG. 5. Areas of equal probabilities (sorting v_{10} then v_{11}).

650.9 for (v_{10}, v_{11}) and 2565.8 for (v_{15}, v_{16}) . The large number in the latter case is related to the fact that (v_{15}, v_{16}) is the pair of ϕ, ψ angles around the C_α atom of Phe-4, for which positive ϕ values are disallowed [18].

The RM_2 scheme which we have tested adds updates for the three pairs (v_7, v_8) , (v_{10}, v_{11}) , and (v_{15}, v_{16}) after one-angle updates for all 24 angles with the RM_1 scheme. For each pair both orders of sorting are used, so that we add altogether six new updates. The bookkeeping for this process is a bit tricky, because an accepted update changes not only $(j, k) \rightarrow (j', k')$, but also the j from the RM_1 updating of the angles. The latter corresponds to a different table and needs to be recalculated from the new value of the angle. As already mentioned, this can be done in $\log_2(n_{\text{tab}})$ steps [9]. Similarly, accepted RM_1 updates can change the initial RM_2 (j, k) values, so that they may have to be recalculated. The six RM_2 update tables, each of size 16×16 , are built from the 400 K Metropolis simulation, and the areas of four of them are precisely those shown in Figs. 3–6.

Numerical results

We have checked the correctness of our updating procedure by comparing high-precision energy averages and other observables with results from previous calculations. The acceptance rates of the one-variable updates remain the same as they were for the RM_1 procedure. For the acceptance rate

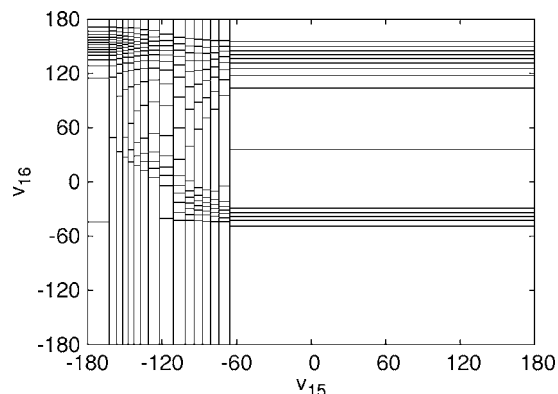
FIG. 6. Areas of equal probabilities (sorting v_{15} then v_{16}).

TABLE IV. Acceptance rates for simultaneous moves of angle pairs.

| Variable pair | 400 K | 300 K | 300 K | 300 K |
|--------------------|-------|--------|---------------------|----------------------|
| | Metro | Metro | RM ₂ | RM ₂ |
| | | | $n_{\text{tab}}=16$ | $n_{\text{tab}}=128$ |
| (v_7, v_8) | 0.044 | 0.0060 | 0.019 | 0.020 |
| (v_{10}, v_{11}) | 0.041 | 0.0051 | 0.021 | 0.022 |
| (v_{15}, v_{16}) | 0.018 | 0.0051 | 0.048 | 0.050 |

of a pair we average over the two cases. Table IV compares the two-angle RM₂ acceptance rates at 300 K to those obtained by proposing the same two-angle updates with the standard Metropolis procedure. At 300 K an increase by factors in the range from 3 to nearly 10 is found. However, the values remain surprisingly low, presumably due to substantial correlations with additional angles.

Integrated autocorrelation times are calculated to evaluate the improvement of the overall performance. For this purpose the number of sweeps between measurements is reduced from 32 to 26 to account for the additional CPU time needed for the two-angle moves. The results are presented in Table II. Despite the small acceptance rates for the two-angle moves, the integrated autocorrelation times for the targeted angles are substantially reduced. For all the six angles they are smaller by factors larger than 2 when compared with the RM₁ results. Interestingly this speed-up propagates through the entire system and the integrated autocorrelation time for the energy is found to be about a factor of 2 smaller than for the RM₁ algorithm.

Multihit updates allow us to focus even more on the angles with large autocorrelation times. For the one-angle updates we use the same numbers of hits as for RM₁ updating (see Table III). In addition we use four hits for the pairs (v_7, v_8) and (v_{10}, v_{11}) and two hits for the (v_{15}, v_{16}) pair. For each pair both orders of the updating are used. Altogether we perform 39 one-angle and 20 two-angle hits per sweep, which is balanced by reducing the number of sweeps between measurements to 13 (the integer nearest to $32 \times 24/59$). The results for integrated autocorrelation times are a mixed bag (compare the last columns of Tables II and III). While the values for the targeted angles indeed go down, in particular for v_8 , the improvement does not propagate to the energy.

In Tables V and VI we present results down to 220 K for the multihit improved Metropolis and RM₂ algorithms, where the distribution of hits is the same as listed in Table III. We always construct the RM₂ table from the previous RM₂ runs at the next higher temperature. We also generate RM₂ data without using the multihit scheme, with the resulting autocorrelation times consistently higher than those reported in Table VI. We have not listed the angles $v_2, v_3, v_4, v_{14}, v_{19}, v_{20}, v_{21}$, and v_{24} in Tables V and VI, because they are not significantly correlated with the rest of the molecule.

When lowering the temperature towards 220 K, the autocorrelation times increase rapidly. To control τ_{int} we double the number of sweeps between measurements each time, when decreasing the temperature. So it is 64 at 280 K, 128 at

TABLE V. Multihit Metropolis at low temperatures.

| Var | 48 | 280 K | 260 K | 240 K | 220 K |
|----------|------|------------|------------|------------|------------|
| | hits | | | | |
| v_1 | 2 | 24.5 (1.7) | 59.8 (4.8) | 246 (18) | 658 (60) |
| v_5 | 3 | 70.7 (5.0) | 236 (27) | 531 (47) | 1672 (148) |
| v_6 | 1 | 34.8 (2.4) | 65.0 (4.8) | 185 (10) | 453 (28) |
| v_7 | 4 | 156 (16) | 526 (88) | 1425 (118) | 4434 (405) |
| v_8 | 4 | 191 (17) | 627 (78) | 1591 (135) | 4965 (485) |
| v_9 | 2 | 60.2 (5.0) | 114 (06) | 467 (33) | 1809 (219) |
| v_{10} | 4 | 186 (15) | 613 (69) | 1530 (131) | 5326 (443) |
| v_{11} | 4 | 214 (18) | 625 (82) | 1901 (148) | 5781 (437) |
| v_{12} | 2 | 20.1 (1.1) | 44.3 (3.2) | 158 (08) | 557 (44) |
| v_{13} | 1 | 15.7 (05) | 36.8 (2.9) | 119 (07) | 279 (17) |
| v_{15} | 4 | 239 (90) | 308 (31) | 999 (78) | 2283 (170) |
| v_{16} | 4 | 204 (12) | 449 (34) | 1600 (129) | 4537 (344) |
| v_{17} | 1 | 11.9 (0.7) | 22.8 (1.2) | 78.8 (2.7) | 278 (15) |
| v_{18} | 1 | 24.1 (2.6) | 55.5 (3.6) | 208 (11) | 755 (46) |
| v_{22} | 2 | 64.5 (4.7) | 136 (10) | 343 (16) | 898 (54) |
| v_{23} | 1 | 37.2 (1.8) | 84.4 (5.1) | 360 (26) | 830 (63) |
| E | | 71.6 (4.0) | 148 (08) | 484 (29) | 1536 (121) |

260 K, 256 at 240 K, and 512 at 220 K. For the multihit Metropolis simulations this was still not sufficient and we performed two additional runs, with 4×256 sweeps at 240 K and with 4×512 sweeps at 220 K. This explains the relatively small error bars in the last two columns of Table V. In the tables we continue to report τ_{int} in units of 32 sweeps, multiplying the measured $\tau_{\text{int}}/32$ value with the number of sweeps between measurements. It is seen that even for the

TABLE VI. RM₂ multihit at low temperatures.

| Var | 39 | 280 K | 260 K | 240 K | 220 K |
|----------|------|------------|------------|------------|------------|
| | hits | | | | |
| v_1 | 1 | 11.6 (0.7) | 27.5 (1.2) | 81.6 (6.2) | 188 (017) |
| v_5 | 2 | 36.9 (1.8) | 89.5 (7.4) | 256 (26) | 824 (103) |
| v_6 | 1 | 10.7 (0.6) | 20.1 (0.7) | 50.4 (2.4) | 146 (017) |
| v_7 | 4 | 45.0 (3.1) | 105 (05) | 359 (27) | 1434 (164) |
| v_8 | 4 | 63.0 (4.0) | 131 (07) | 459 (42) | 2266 (309) |
| v_9 | 1 | 17.5 (0.8) | 44.9 (1.9) | 130 (10) | 405 (030) |
| v_{10} | 4 | 59.9 (4.1) | 134 (09) | 514 (57) | 2344 (300) |
| v_{11} | 4 | 57.1 (3.6) | 157 (10) | 495 (35) | 1965 (178) |
| v_{12} | 1 | 8.04 (30) | 20.1 (1.0) | 52.9 (3.4) | 131 (008) |
| v_{13} | 1 | 6.55 (25) | 12.9 (0.7) | 39.0 (3.5) | 86.7 (6.8) |
| v_{15} | 2 | 43.5 (6.4) | 88.8 (4.9) | 265 (18) | 775 (082) |
| v_{16} | 2 | 58.7 (2.8) | 140 (08) | 420 (32) | 1569 (164) |
| v_{17} | 1 | 4.43 (20) | 9.72 (44) | 30.7 (1.9) | 69.2 (4.4) |
| v_{18} | 1 | 10.7 (0.5) | 26.5 (1.2) | 65.6 (2.6) | 206 (12) |
| v_{22} | 1 | 25.4 (1.3) | 53.6 (2.7) | 124 (05) | 281 (014) |
| v_{23} | 1 | 11.6 (0.6) | 28.2 (1.7) | 88.2 (5.2) | 267 (022) |
| E | | 22.9 (1.1) | 47.9 (1.8) | 128 (09) | 426 (038) |

RM₂ simulation the τ_{int} increases are not compensated by the increase of computer time. In contrast to that, the decrease in acceptance rates is rather moderate, less than a factor of 2 when the temperature is lowered from 300 K to 220 K.

The results of Tables V and VI show that our RM₂ sampling accelerates the conventional Metropolis simulations by a rather temperature-independent factor. As we can assume that the multihit Metropolis simulations already improve conventional Metropolis simulations by about 40%, the RM₂ acceleration is by a factor between 4 and 5 with respect to a conventional Metropolis simulation. For large-scale simulations factors larger than 2 are clearly of importance, but it remains a bit puzzling why the improvement does not increase upon lowering the temperature, as is found when using generalized ensembles. Apparently coordinated moves of three and more angles are needed.

IV. SUMMARY AND CONCLUSIONS

We have reviewed the one-variable approximation RM₁ of the rugged Metropolis scheme of Ref. [1] and worked out a two-variable approximation RM₂ for simultaneous moves of two dihedral angles. As before the test system has been Met-Enkephalin. A gain of a factor of 4 over conventional Metropolis simulations has been demonstrated at 300 K.

Although the elaboration of the RM scheme seems to be on track, much work is left to be done. Even for a system as simple as Met-Enkephalin it remains unclear which kinds of correlations are responsible for the still low acceptance rates of the two-angles moves. On the other hand, it is encouraging to see that the autocorrelations times of these angles are nevertheless substantially reduced and that this effect propagates through the entire system. Other test cases need to be investigated to get a broader understanding of the observed features. In particular one would like to know how the performance gain depends on the system size.

Somewhat puzzling is the lack of enhanced improvements at lower temperatures. The real future of biased updating

procedures may lie in their implementation for generalized ensembles.

Presently the leading method for simulations of biomolecules is molecular dynamics (see [19] for a textbook). This is to some extent surprising, because Markov-chain Monte Carlo simulations allow for large changes of conformations in a single move, so thermodynamically relevant equilibrium configurations can, in principle, be reached quickly. However, in simulations of biomolecules with an explicit inclusion of solvent interactions, large MC moves face the problem that there will not be a suitable cavity in the solvent to accommodate a large distortion of the molecule shape. While the RM method discussed in this paper decreases the likelihood of steric clashes in a vacuum simulation, it has no immediate translation into the situation of explicit solvent models.

The way out may be the use of implicit solvent models, for which the change in the molecule-solvent and solvent-solvent interaction energies can be calculated instantaneously, like in a vacuum simulation. Indeed RM₁ simulations for implicit solvent models, based on the solvent-accessible area method implemented in [17], have already been performed [20]. The algorithmic improvements were similar as found for the vacuum situation. However, there is evidence [20,21] that the class of solvent models used does not parametrize the solvent interactions properly. It appears that quite generally the reliability of implicit solvent models has not yet been well established.

Finally we like to mention that MC moves may be fine-tuned on a local level as done in the approach of Ref. [22]. This is also possible for models which include solvents explicitly. So MC simulations may still be a viable alternative to molecular dynamics for explicit solvent models.

ACKNOWLEDGMENTS

Our calculations were performed on the Anfinen PC cluster of FSU's School of Computational Science. H.-X.Z. was supported in part by National Institutes of Health Grant No. GM 58187.

-
- [1] B. A. Berg, *Phys. Rev. Lett.* **90**, 180601 (2003).
 [2] D. Bryngelson and P. G. Wolynes, *Proc. Natl. Acad. Sci. U.S.A.* **84**, 7524 (1987).
 [3] W. K. Hastings, *Biometrika* **57**, 97 (1970).
 [4] A. D. Bruce, *J. Phys. A* **18**, L873 (1985).
 [5] A. Milchev, D. W. Heermann, and K. Binder, *J. Stat. Phys.* **44**, 749 (1986).
 [6] M. W. Deem and J. S. Bader, *Mol. Phys.* **87**, 1245 (1996).
 [7] G. Favrin, A. Irbäck, and F. Sjunnesson, *J. Chem. Phys.* **114**, 8154 (2001).
 [8] J. P. Ulmschneider and W. L. Jorgensen, *J. Chem. Phys.* **118**, 4261 (2003).
 [9] A. Bazavov and B. A. Berg, *Phys. Rev. D* **71**, 114506 (2005).
 [10] G. La Penna, S. Morante, A. Perico, and G. C. Rossi, *J. Chem. Phys.* **121**, 10725 (2004); B. Berg, H. Noguchi, and Y. Okamoto, *Phys. Rev. E* **68**, 036126 (2003); U. H. E. Hansmann, *Physica A* **321**, 152 (2003); A. Mitsutake, Y. Sugita, and Y. Okamoto, *Biopolymers* **60**, 96 (2001).
 [11] N. Go and H. A. Scheraga, *Macromolecules* **3**, 178 (1970).
 [12] Z. Li and H. A. Scheraga, *Proc. Natl. Acad. Sci. U.S.A.* **85**, 6611 (1987).
 [13] U. H. Hansmann, M. Masuya, and Y. Okamoto, *Proc. Natl. Acad. Sci. U.S.A.* **94**, 10652 (1997).
 [14] N. A. Alves and U. H. Hansmann, *Int. J. Mod. Phys. C* **11**, 301 (2000).
 [15] B. A. Berg, *Markov Chain Monte Carlo Simulations and Their Statistical Analysis* (World Scientific, Singapore, 2004).
 [16] M. J. Sippl, G. Nemethy, and H. A. Scheraga, *J. Chem. Phys.* **88**, 6231 (1984) and references given therein.
 [17] F. Eisenmenger, U. H. Hansmann, S. Hayryan, and C.-K. Hu, *Comput. Phys. Commun.* **138**, 192 (2001).
 [18] G. E. Schultz and R. H. Schirmer, *Principle of Protein Struc-*

- ture* (Springer, New York, 1979).
- [19] D. Frenkel and B. Smit, *Understanding Molecular Simulation* (Academic Press, San Diego, 1996).
- [20] B. A. Berg and H.-P. Hsu, Phys. Rev. E **69**, 026703 (2004).
- [21] Y. Peng, U. H. Hansmann, and N. A. Alves, J. Chem. Phys. **118**, 2374 (2003); Y. Peng and U. H. Hansmann, Biophys. J. **82**, 3269 (2003).
- [22] D. Bouzida, S. Kumar, and R. Swendsen, Phys. Rev. A **45**, 8894 (1992).